

Algorithm-independent bounds on complex optimization through the statistics of marginal optima

Jaron Kent-Dobias*

Istituto Nazionale di Fisica Nucleare, Sezione di Roma I, Rome, Italy 00184

Optimization seeks extremal points in a function. When there are superextensively many optima, optimization algorithms are liable to get stuck. Under these conditions, generic algorithms tend to find marginal optima, which have many nearly flat directions. In a companion paper, we introduce a technique to count marginal optima in random landscapes. Here, we use the statistics of marginal optima calculated using this technique to produce generic bounds on optimization, based on the simple principle that algorithms will overwhelmingly tend to get stuck only where marginal optima are found. We demonstrate the idea on a simple non-Gaussian problem of maximizing the sum of squared random functions on a compact space. Numeric experiments using both gradient descent and generalized approximate message passing algorithms fall inside the expected bounds.

In optimization one usually looks for the global maximum or minimum of an objective or energy function. Whether this is possible or likely depends on the structure of the particular problem. Many optimization problems are understood to have three phases: an easy phase, where a good global solution can be quickly found by a well-chosen algorithm; an impossible phase, where no such solution exists; and a hard phase, where a proliferation of bad local solutions make the search for the good global one interminable [1, 2].

In the hard phase, the bad local optima found by algorithms are not completely random: in the large-problem limit, the same algorithm run many times on many statistically identical systems finds optima with the same properties. For a long time physicists believed that many algorithms would find optima at a special energy level, the threshold energy E_{th} , where level sets of the energy transition from containing mostly saddles to containing mostly minima. Recent work has shown that this is not actually true [3–5]. However, there is a kernel of truth in the old idea.

As the transition point in energy between mostly saddles and mostly minima, the threshold energy itself is characterized by mostly *marginal minima*, which are minima whose Hessian has a pseudogap and that therefore have many nearly flat directions [6]. While the threshold energy is now understood to not be a meaningful attractor of dynamics, marginal minima appear to be robust attractors of dynamics across a wide variety of models and algorithms. There are multiple, complimentary ways to understand why this might be so. On one hand, their flat directions make their basins of attraction naïvely much larger than those of minima with only stiff directions. On the other, marginal minima can gregariously accumulate along their flat directions, giving rise to large flat regions that are likewise easy to find [7–9]. However, these intuitions cannot be understood to form a proof; rather, the attractiveness of marginal minima is right now an empirical observation.

This empirical fact is now fairly well established among a variety of hard models under a variety of algorithms [10–13]. Gradient flow and descent, stochastic gradient descent, Langevin or Monte Carlo annealing all find asymptotically

marginal minima in many complex landscapes. This is also true of approximate message passing algorithms whose dynamics runs outside configuration space but nonetheless end at marginal minima. The exceptions to this rule are few and represent non-generic methods. For instance, stiff solutions to random XORSAT can be found by a nonlocal and non-generic change of variables that renders the transformed problem easy [14]. And of course, any problem in its easy phase finds the good solution whether it is stiff or not.

Taking the inevitability of marginal minima as a fact, one can try to derive effective bounds on performance by inverting the logic: if generic algorithms in complex settings find marginal optima, then the range of performances of generic algorithms must lie in the range of energies in which marginal optima can be found. This motivates the study of marginal optima and their properties independent of our algorithm of interest. In our companion paper, we introduce a general technique for studying the properties of marginal optima [15]. Here, we will use these results to test the relationship between the distribution of marginal optima and the performance of algorithms in a family of simple non-Gaussian energy landscapes.

Consider the problem of maximizing the sum of squared random functions constrained to a manifold. In this case, the energy to minimize is minus the sum of squares

$$H(\mathbf{x}) = -\frac{1}{2} \sum_{k=1}^M V_k(\mathbf{x})^2 \quad (1)$$

of $M = \alpha N$ centered Gaussian random functions V_k . The configurations $\mathbf{x} \in \mathbb{R}^N$ are constrained to lie on the hypersphere $\|\mathbf{x}\|^2 = N$. The functions V_k are defined such that their covariance at two different points \mathbf{x}, \mathbf{x}' is

$$\overline{V_i(\mathbf{x})V_j(\mathbf{x}')^2} = N\delta_{ij}f\left(\frac{\mathbf{x} \cdot \mathbf{x}'}{N}\right) \quad (2)$$

for some function f with positive series coefficients. Each V_k can be understood as consisting of sums of fully connected, independently normally distributed p -term interactions between the components of \mathbf{x} whose variance is proportional to $f^{(p)}(0)$, the p th series coefficient of f .

This problem has been studied recently because of its resemblance to other problems in physics, mathematics, and

* jaron.kent-dobias@roma1.infn.it

optimization, like nonlinear least squares and vertex models of tissues [16–26]. However, those motivations favor the opposite optimization problem of minimizing the sum of squares, or equivalently maximizing H . Unfortunately minimizing the sum of squares in this model is a poor platform to test the idea introduced in this paper. This previous research suggests that for many choices of f the problem of minimizing the sum of squares is characterized by global and near-global optima belonging to a wide flat manifold, the signature of so-called full replica symmetry breaking (RSB) order. Not only are such cases more difficult to treat analytically, but they also often *easy* for certain algorithms [27]. The problem of maximizing the sum of squares, or minimizing H , instead is typically characterized by isolated solutions belonging to the *hard* family of 1RSB problems. Motivated by our goal of producing bounds for performance in the hard regime, we will study the relationship between marginal minima of H and the performance of algorithms.

In the physics of spin glasses there are a well-worn set of tools for studying the statistics of optima in certain kinds of random hard problems. In such problems, the number of optima $\mathcal{N}_H(E)$ at a certain energy level $E = H/N$ is typically exponentially large in the size N of the problem. The reliable measure of typical statistics of optima is therefore the average of the logarithm this number, which defines the complexity $\Sigma(E) = \frac{1}{N} \log \mathcal{N}_H(E)$. When the complexity Σ is positive there are typically exponentially many optima, while when it is negative it is extremely unlikely to find any.

Remarkably, this typical count can be computed in a variety of fully-connected models, including by a method which involves a Legendre transformation of a mere equilibrium calculation [28]. A more flexible approach is offered by an old technique called the Kac–Rice method [29, 30]. Here, the number of optima is found by integrating a Dirac δ function containing the gradient over configuration space, weighted by a Jacobian that consists of the Hessian:

$$\mathcal{N}_H(E) = \int d\mathbf{x} \delta(\nabla H(\mathbf{x})) |\det \text{Hess } H(\mathbf{x})| \delta(NE - H(\mathbf{x})) \quad (3)$$

The use of this method in the statistical physics of random landscapes is well established in diverse settings [31–34].

Unfortunately these traditional approaches are not sufficient for the purposes of characterizing marginal optima. The typical complexity $\Sigma(E)$ corresponds with the statistics of

marginal minima only at the threshold energy E_{th} . For smaller energies it characterizes stiff minima, while for larger energies it characterizes unstable saddle points. To characterize the typical complexity of marginal minima $\Sigma_m(E)$, we need to condition the count of stationary points on their marginality. Both traditional approaches to calculating the complexity present unique problems. In the Kac–Rice approach, conditioning on marginality requires a complicated condition on the Hessian of the energy at a stationary point. In all but Gaussian landscapes, properties of the Hessian at a point are dependent on its stationarity and energy [35, 36]. Characterizing the Hessian at stationary points in non-Gaussian problems is a class of calculation just in its infancy [37]. Further conditioning the problem using the result of such a calculation is further still. On the other hand, the Legendre transform technique does not offer obvious ways to add further conditions on the properties of the stationary points being counted.

In our companion paper, we introduce a method for calculating the marginal complexity that avoids these problems by sidestepping the need to thoroughly understand the spectral problems of the conditioned Hessian [15]. This method has two steps: first, we insert in the integral (3) a resolution of a Dirac δ function that conditions the smallest eigenvalue λ_{\min} of the Hessian to take a specific value λ^* . Of course, marginal minima correspond with $\lambda^* = 0$, but the converse is not necessarily true: spectra with isolated atoms at zero satisfy this but are not marginal. Therefore, a second step is necessary to ensure the conditioned minima are marginal.

We further condition the count on the fact that $\text{Tr Hess } H = N\mu$, i.e., that the trace of the Hessian is fixed to a specific value. When μ is large and $\lambda^* = 0$, the spectra of typical points have a continuous bulk which is positive and an isolated atom at zero. When μ is decreased far enough, the bulk of the spectrum will hit zero and the large-deviation calculation that corresponds to fixing the lowest eigenvalue will break down, producing imaginary predictions. By adjusting μ and looking for this breakdown, we can tune the spectrum of stationary points to have a pseudogap, and therefore be marginal, without actually understanding the form of the bulk spectrum. At each energy we expect a different value $\mu_m(E)$ of the trace to reach this marginal point.

In the companion paper, we calculate the λ^* - and μ -dependent complexity of optima in the maximum of sum of squares problem under the assumption that its structure is 1RSB. The result takes the form of an extremal problem

$$\begin{aligned} \Sigma_{\lambda^*}(E, \mu) = & \underset{\hat{\beta}, \hat{\lambda}, r, d, g, y, \Delta z}{\text{extremum}} \left[\hat{\beta}E - \mu(r + g + \hat{\lambda}) + \hat{\lambda}\lambda^* + \frac{1}{2} \log \left(\frac{d + r^2}{g^2} \times \frac{y^2 - 2\Delta z}{y^2} \right) \right. \\ & \left. - \frac{\alpha}{2} \log \left(\frac{1 - 2(2y + \hat{\lambda})f'(1) + 4(y^2 - 2\Delta z)f'(1)^2}{[1 - 2yf'(1)]^2} \times \frac{f(1)[f'(1)d - \hat{\beta} - f''(1)(r^2 - g^2 + 8(y\hat{\lambda} + \Delta z) + 2\hat{\lambda}^2)] + [1 - rf'(1)]^2}{[1 + gf'(1)]^2} \right) \right] \quad (4) \end{aligned}$$

In problems like the one considered here, which have all noise

and no signal, there is another simplification. Under these cir-

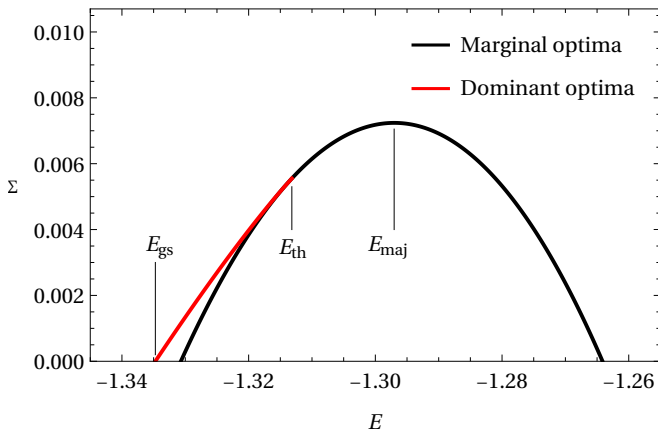


FIG. 1. The marginal and dominant complexities of the random sum of squares problem with $\alpha = \frac{1}{8}$ and covariance function $f(q) = \frac{1}{4}q + \frac{3}{4}q^2$. Several important energies are marked on the plot: the ground state energy E_{gs} where the lowest optima are found, the threshold energy E_{th} where marginal optima are the most common kind of optima, and the majority energy E_{maj} where most marginal optima are found.

cumstances, typical minima do not have isolated eigenvalues, and pulling one out of the continuous part of the spectrum always decreases the complexity. Therefore, the complexity resulting from fixing the minimum eigenvalue λ^* to be at the bottom edge of the bulk spectrum will be stationary with respect to the position of the eigenvalue, or $0 = \frac{\partial}{\partial \lambda^*} \Sigma_{\lambda^*}(E, \mu)$. We can thus choose the marginal trace $\mu_m(E)$ as the value of μ such that the complexity is stationary with respect to variation of the minimum eigenvalue about zero, or by solving

$$0 = \left. \frac{\partial}{\partial \lambda^*} \Sigma_{\lambda^*}(E, \mu_m(E)) \right|_{\lambda^*=0}. \quad (5)$$

for $\mu_m(E)$. This allows us to define the marginal complexity $\Sigma_m(E) = \Sigma_0(E, \mu_m(E))$ in a purely variational way.

Combining the λ^* -dependent complexity (4) with the requirement (5) allows us to compute the marginal complexity for the problem of maximizing sums of squared random functions. This is plotted as a function of energy E in comparison to the dominant complexity for a representative example of the maximum random sum of squares problem in Fig. 1. That figure shows several features that are ubiquitous in optimizing hard complex problems. Indeed, they are ubiquitous enough features that this plot appears schematically almost identical to that of [Folena et al.](#) for the Gaussian spherical spin glasses, despite relying on a more sophisticated calculation [3]. First, marginal minima are found in exponential number at energies far above the threshold energy, which a naïve analysis of the dominant complexity might lead one to conclude is the highest energy at which minima can be found. Second, there is a gap in energy between the lowest marginal minima and the ground state. This is a gulf that one cannot hope to cross with a generic algorithm.

How does the performance of real algorithms compare with

these broad bounds? We studied this question by performing two prototypical algorithms for complex optimization: gradient descent and generalized approximate message passing. The first, gradient descent, starts at a random point in configuration space and takes strictly downward steps in the direction of the gradient whose magnitude is determined by a simple line search. The second, generalized approximate message passing, was introduced for the spherical spin glasses under another name and in a slightly different form by [Subag](#) [38, 39]. This algorithm starts outside of configuration space with a unit vector in a random direction. Every step is a unit vector in the direction of the gradient but orthogonal to the current state. After N such steps, the configuration lies on the radius \sqrt{N} hypersphere. In order to ensure that the resulting configuration is a minimum, we afterwards run gradient descent using this configuration as the starting condition. In the Gaussian spherical spin glasses this algorithm has been proven to be asymptotically optimal among a broad class of generic algorithms [39]. In the present non-Gaussian problem of maximizing random sums of squares it is not known whether it is optimal, but our experiments indicate that it usually outperforms gradient descent.

We ran these algorithms on independent random instances of the maximum sum of squares problem with $\alpha = \frac{1}{8}$ and covariance functions $f(q) = \kappa q + (1 - \kappa)q^2$ for a variety of κ between zero and one and for a variety of system sizes between $N = 16$ and 2048. First, we confirmed that both algorithms indeed find asymptotically marginal minima by calculating the average of the smallest eigenvalue of the Hessian $\lambda_{\min}(N)$ as a function of system size. As expected, this smallest eigenvalue asymptotically approaches zero as N becomes large, and we measured power law scaling. We further found that the energy achieved asymptotically approaches its infinite-size value with a power law whose exponent depends on κ . Details of our numeric analysis can be found in the supplementary material.

The asymptotic results of these numeric experiments are compared with the predictions of the marginal complexity in Fig. 2. The range of energies where marginal complexity is positive succeed at effectively bounding the algorithmic performance over the entire range of models, though often the bound is not very tight. The threshold energy E_{th} is often not asymptotically reached by gradient descent and is usually beaten by message passing; as for the spherical spin glasses, it doesn't have a straightforward relationship with algorithmic performance, though it is possibly a lower bound for gradient descent from a random initial condition [5]. In this family of models and for the spherical spin glasses, the energy E_{maj} at which the majority of marginal minima are found may be an effective upper bound on the performance of gradient descent, but we do not have a principled reason for this.

In this paper, we have demonstrated on a non-Gaussian complex optimization problem that the complexity of marginal minima can be used to effectively bound algorithmic performance independent of the algorithm used. The computation of this marginal complexity in the non-Gaussian case was made possible by the techniques introduced in our companion paper.

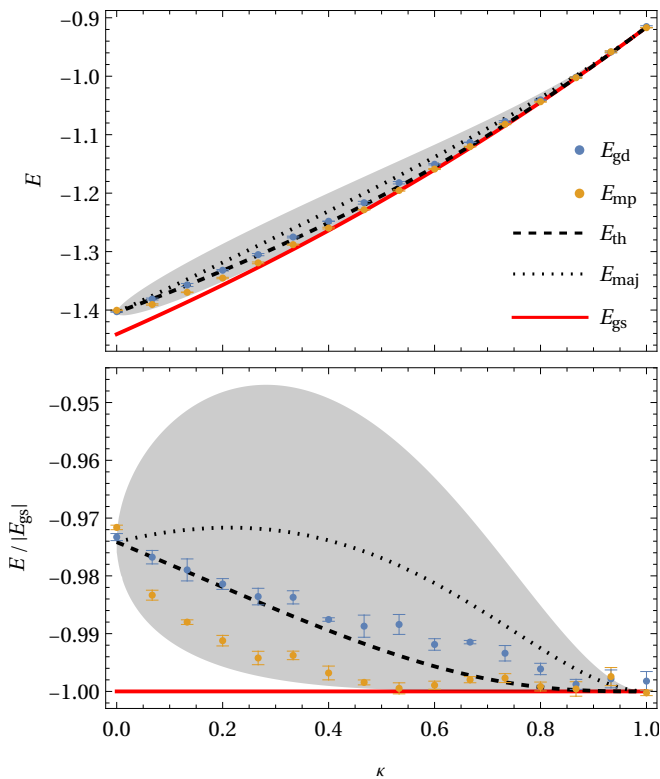


FIG. 2. Comparison of the marginal complexity with the asymptotic performance of gradient descent (E_{gd}) and generalized approximate message passing algorithms (E_{mp}) for maximum sum of squares models with $\alpha = \frac{1}{8}$ and covariance function $f(q) = \kappa q + (1 - \kappa)q^2$ as κ is varied. The shaded region shows the range of energies at which the marginal complexity is positive. The lines indicated on the legend show the threshold energy, majority energy, and ground state energy. The bottom plot is a rescaling of the top plot by the ground state energy to make the comparison with marginal complexity easier. Error bars show one standard error.

When comparing with algorithmic performance in a ‘worst case’ (gradient descent) and ‘best case’ (generalized approximate message passing), the bounds set by marginal complexity are followed, albeit often loosely.

Despite being loose, the bounds derived by marginal complexity represent a useful development. The method used to compute the marginal complexity introduced in our companion paper is general and should be applied to other systems in much the same way as equilibrium calculations, despite being more complex than an equilibrium calculation. The current rigorous and often tight lower bounds on performance developed for spin glass models using the overlap gap property have yet to be generalized to non-Gaussian continuous models [27, 40, 41]. It is also an open question, even in simple spherical spin glasses, at what energy the ‘worst case’ of gradient flow arrives. This means that marginal complexity can make a initial, perhaps loose, lower *and* upper bound on behavior without needing to develop substantially new model-specific approaches.

Some future development of the method is necessary for ef-

ficiently applying it to systems with a nonzero signal. In such cases, there are circumstances where typical stationary points have an isolated eigenvalue, and the variational approach of (5) for finding the shift of the spectrum corresponding to a pseudogap will fail [33]. While we described a generic method for doing this by looking for the breakdown of the large-deviation principle behind the calculation, an extended variational approach would be much easier to work with. It is possible something of this kind could be accomplished by treating the signal direction and the directions orthogonal to it separately.

The numeric comparisons made in this paper were constrained to small powers of q in $f(q)$ and to small α by the computational feasibility of getting sufficient statistics from the simulations. With use of the dynamical mean field theory results already developed for the sum of squared random functions, comparisons with asymptotic dynamics should be made for a wider range of model parameters [22, 23]. Further development of the marginal complexity in the full rsb setting for comparison with the least squares problem should also be made.

In order to improve the bounds made by marginal complexity, it would be beneficial to understand if there is something structural about the type of marginal minima that can attract some algorithmic dynamics and those that cannot attract any. Recent analysis of the two-point complexity of marginal minima in the spherical models did not find such a signature [42]. It was recently proposed that traits related to the self-similarity and stochastic stability of minima might be important, but these ideas are still in their infancy [24].

JK-D is supported by a DYN SYS MATH Specific Initiative of the INFN. The authors thank James P Sethna, Ralph B Robinson, and Bethany Dixon at Cornell University for providing and facilitating access to computing resources used in this work.

-
- [1] L. Zdeborová and F. Krzakala, Statistical physics of inference: thresholds and algorithms, *Advances in Physics* **65**, 453 (2016).
 - [2] D. Gamarnik, C. Moore, and L. Zdeborová, Disordered systems insights on computational hardness, *Journal of Statistical Mechanics: Theory and Experiment* **2022**, 114015 (2022).
 - [3] G. Folena, S. Franz, and F. Ricci-Tersenghi, Rethinking mean-field glassy dynamics and its relation with the energy landscape: The surprising case of the spherical mixed p -spin model, *Physical Review X* **10**, 031045 (2020).
 - [4] G. Folena, S. Franz, and F. Ricci-Tersenghi, Gradient descent dynamics in the mixed p -spin spherical model: finite-size simulations and comparison with mean-field integration, *Journal of Statistical Mechanics: Theory and Experiment* **2021**, 033302 (2021).
 - [5] G. Folena and F. Zamponi, On weak ergodicity breaking in mean-field spin glasses, *SciPost Physics* **15**, 109 (2023).
 - [6] M. Müller and M. Wyart, Marginal stability in structural, spin, and electron glasses, *Annual Review of Condensed Matter Physics* **6**, 177 (2015).
 - [7] C. Baldassi, C. Borgs, J. T. Chayes, A. Ingrosso, C. Lucibello, L. Saglietti, and R. Zecchina, Unreasonable effectiveness of

- learning neural networks: From accessible states and robust ensembles to basic algorithmic schemes, *Proceedings of the National Academy of Sciences* **113**, E7655 (2016).
- [8] C. Baldassi, C. Lauditi, E. M. Malatesta, G. Perugini, and R. Zecchina, Unveiling the structure of wide flat minima in neural networks, *Physical Review Letters* **127**, 278301 (2021).
- [9] C. Baldassi, E. M. Malatesta, G. Perugini, and R. Zecchina, Typical and atypical solutions in nonconvex neural networks with discrete and continuous weights, *Physical Review E* **108**, 024310 (2023).
- [10] G. Parisi, On the statistical properties of the large time zero temperature dynamics of the SK model, [arXiv:cond-mat/9501045v1](https://arxiv.org/abs/cond-mat/9501045v1) (1995).
- [11] H. Horner, Time dependent local field distribution and metastable states in the SK-spin-glass, *The European Physical Journal B* **60**, 413 (2007).
- [12] V. Erba, F. Behrens, F. Krzakala, and L. Zdeborová, Quenches in the Sherrington-Kirkpatrick model, [arXiv:2405.04267v2](https://arxiv.org/abs/2405.04267v2) (2024).
- [13] G. Folea and P. Urbani, Marginal stability of soft anharmonic mean field spin glasses, *Journal of Statistical Mechanics: Theory and Experiment* **2022**, 053301 (2022).
- [14] L. Foini, F. Krzakala, and F. Zamponi, On the relation between kinetically constrained models of glass dynamics and the random first-order transition theory, *Journal of Statistical Mechanics: Theory and Experiment* **2012**, P06013 (2012).
- [15] J. Kent-Dobias, Conditioning the complexity of random landscapes on marginal optima, [arXiv:2407.02082](https://arxiv.org/abs/2407.02082) [*cond-mat.dismn*] (2024).
- [16] Y. V. Fyodorov, A spin glass model for reconstructing nonlinearly encrypted signals corrupted by noise, *Journal of Statistical Physics* **175**, 789 (2019).
- [17] Y. V. Fyodorov and R. Tublin, Counting stationary points of the loss function in the simplest constrained least-square optimization, *Acta Physica Polonica B* **51**, 1663 (2020).
- [18] Y. V. Fyodorov and R. Tublin, Optimization landscape in the simplest constrained random least-square problem, *Journal of Physics A: Mathematical and Theoretical* **55**, 244008 (2022).
- [19] R. Tublin, *A Few Results in Random Matrix Theory and Random Optimization*, Ph.D. thesis, King's College London (2022).
- [20] P. Vivo, Random linear systems with quadratic constraints: from random matrix theory to replicas and back, [arXiv:2401.03209v2](https://arxiv.org/abs/2401.03209v2) (2024).
- [21] P. Urbani, A continuous constraint satisfaction problem for the rigidity transition in confluent tissues, *Journal of Physics A: Mathematical and Theoretical* **56**, 115003 (2023).
- [22] P. J. Kamali and P. Urbani, Stochastic gradient descent outperforms gradient descent in recovering a high-dimensional signal in a glassy energy landscape, [arXiv:2309.04788v2](https://arxiv.org/abs/2309.04788v2) (2023).
- [23] P. J. Kamali and P. Urbani, Dynamical mean field theory for models of confluent tissues and beyond, *SciPost Physics* **15**, 219 (2023).
- [24] P. Urbani, Statistical physics of complex systems: glasses, spin glasses, continuous constraint satisfaction problems, high-dimensional inference and neural networks, [arXiv:2405.06384v1](https://arxiv.org/abs/2405.06384v1) (2024).
- [25] A. Montanari and E. Subag, Solving overparametrized systems of random equations: I. model and algorithms for approximate solutions, [arXiv:2306.13326v1](https://arxiv.org/abs/2306.13326v1) (2023).
- [26] A. Montanari and E. Subag, On Smale's 17th problem over the reals, [arXiv:2405.01735v1](https://arxiv.org/abs/2405.01735v1) (2024).
- [27] D. Gamarnik, The overlap gap property: A topological barrier to optimizing over random structures, *Proceedings of the National Academy of Sciences* **118**, e2108492118 (2021).
- [28] R. Monasson, Structural glass transition and the entropy of the metastable states, *Physical Review Letters* **75**, 2847 (1995).
- [29] M. Kac, On the average number of real roots of a random algebraic equation, *Bulletin of the American Mathematical Society* **49**, 314 (1943).
- [30] S. O. Rice, The distribution of the maxima of a random curve, *American Journal of Mathematics* **61**, 409 (1939).
- [31] A. Cavagna, I. Giardina, and G. Parisi, An investigation of the hidden structure of states in a mean-field spin-glass model, *Journal of Physics A: Mathematical and General* **30**, 7021 (1997).
- [32] M. Müller, L. Leuzzi, and A. Crisanti, Marginal states in mean-field glasses, *Physical Review B* **74**, 134431 (2006).
- [33] V. Ros, G. Ben Arous, G. Biroli, and C. Cammarota, Complex energy landscapes in spiked-tensor and simple glassy models: Ruggedness, arrangements of local minima, and phase transitions, *Physical Review X* **9**, 011003 (2019).
- [34] J. Kent-Dobias and J. Kurchan, How to count in hierarchical landscapes: a full solution to mean-field complexity, *Physical Review E* **107**, 064111 (2023).
- [35] Y. V. Fyodorov, Complexity of random energy landscapes, glass transition, and absolute value of the spectral determinant of random matrices, *Physical Review Letters* **92**, 240601 (2004).
- [36] A. J. Bray and D. S. Dean, Statistics of critical points of Gaussian fields on large-dimensional spaces, *Physical Review Letters* **98**, 150201 (2007).
- [37] A. Maillard, G. Ben Arous, and G. Biroli, Landscape complexity for the empirical risk of generalized linear models, in *Proceedings of The First Mathematical and Scientific Machine Learning Conference*, Proceedings of Machine Learning Research, Vol. 107, edited by J. Lu and R. Ward (PMLR, 2020) pp. 287–327.
- [38] E. Subag, Following the ground states of full-RSB spherical spin glasses, *Communications on Pure and Applied Mathematics* **74**, 1021 (2020).
- [39] A. El Alaoui, A. Montanari, and M. Sellke, Optimization of mean-field spin glasses, *The Annals of Probability* **49**, 2922 (2021).
- [40] D. Gamarnik and A. Jagannath, The overlap gap property and approximate message passing algorithms for p -spin models, *The Annals of Probability* **49**, 180 (2021).
- [41] B. Huang, *Computational Hardness in Random Optimization Problems from the Overlap Gap Property*, Ph.D. thesis, Massachusetts Institute of Technology (2022).
- [42] J. Kent-Dobias, Arrangement of nearby minima and saddles in the mixed spherical energy landscapes, *SciPost Physics* **16**, 001 (2024).

Supplement to Algorithm-independent bounds on complex optimization through the statistics of marginal optima

Jaron Kent-Dobias

Istituto Nazionale di Fisica Nucleare, Sezione di Roma I, Rome, Italy 00184

This supplement describes in detail the procedure and analysis of the numeric experiments whose results appear in the main text.

IMPLEMENTATION OF THE ENERGY

Define the projection matrix

$$P_{\mathbf{x}} = I - \frac{\mathbf{x}\mathbf{x}^T}{\|\mathbf{x}\|^2} \quad (1)$$

which projects a vector into the subspace orthogonal to \mathbf{x} . Then the gradient can be derived from the derivative with respect to \mathbf{x} by

$$\nabla H(\mathbf{x}) = P_{\mathbf{x}} \partial H(\mathbf{x}) \quad (2)$$

Likewise the Hessian matrix is

$$\text{Hess } H(\mathbf{x}) = P_{\mathbf{x}} \left[\partial \partial H(\mathbf{x}) - \frac{\mathbf{x}^T \partial H(\mathbf{x})}{N} I \right] P_{\mathbf{x}}^T \quad (3)$$

The Hessian so defined has a zero eigenvalue whose corresponding eigenvector is \mathbf{x} . This must be discarded in any analysis of the stability.

SPECIFICATION OF THE ALGORITHMS

Our gradient descent algorithm is standard, with a simple line search to determine the step size whose acceptance is made with the Wolfe criterion [1]. The algorithm is halted when the squared norm of the gradient falls under a certain threshold ϵN , where we take $\epsilon = 10^{-13}$. The choice for ϵ was made because it is roughly the smallest value possible before some loops hang due to machine imprecision.

Algorithm 1 Gradient descent

```

function NORMALIZE( $\mathbf{x}$ )
  return  $\frac{\sqrt{N}}{\|\mathbf{x}\|} \mathbf{x}$ 
end function
 $\mathbf{x} \leftarrow \mathbf{x}_0$ 
 $\alpha \leftarrow 1$ 
while  $\|\nabla H(\mathbf{x})\|^2 / N > \epsilon$  do
  while  $\mathbf{x}' \leftarrow \text{NORMALIZE}(\mathbf{x} - \alpha \nabla H(\mathbf{x}))$ ,
     $H(\mathbf{x}') > H(\mathbf{x}) - \frac{1}{2} \alpha \|\nabla H(\mathbf{x})\|^2$  do
     $\alpha \leftarrow \frac{1}{2} \alpha$ 
  end while
   $\mathbf{x} \leftarrow \mathbf{x}'$ 
   $\alpha \leftarrow \frac{5}{4} \alpha$ 
end while
return  $\mathbf{x}$ 

```

In its original form, the algorithm introduced by Subag used steps proportional to an eigenvector of the Hessian [2]. However, equivalent asymptotic results have been proven to result from steps along the direction of the gradient. Note that based on our definition of the gradient, the steps are orthogonal to the state σ of the algorithm by construction.

Algorithm 2 Approximate message passing

```

 $\sigma \leftarrow \mathbf{x}_0 / N$ 
while  $\|\sigma\|^2 < N$  do
   $\sigma \leftarrow \sigma - \nabla H(\sigma) / \|\nabla H(\sigma)\|$ 
end while
return  $\sigma$ 

```

After the AMP algorithm has terminated we run gradient descent using its output as the initial condition to ensure that the final result is a minimum. The code implementing these algorithms is freely available [3].

EXPERIMENTS AND RAW DATA

Our numeric experiments consisted of running these algorithms many times on independent realizations of the disorder, and measuring the final energy and the minimum eigenvalue of the Hessian. We made extensive use of GNU Parallel command line tool [4]. Linear algebra manipulations were all done using the Eigen library. Experiments were run for models with $\alpha = \frac{1}{8}$ and $f(q) = \kappa q + (1 - \kappa)q^2$ at 16 values of κ evenly spaced between 0 and 1 inclusive, and for system sizes N at powers of 2 from 16 to 2048. The number of independent experiments at each set of parameters is given in Table I.

Here we share the summary statistics for the raw data in the form of the mean and standard error of the mean. Tables II and III show these statistics for the final energies of gradient descent and AMP, respectively, while Tables IV and V show the same statistics for the minimum eigenvalue of the Hessian for gradient descent and AMP, respectively.

ANALYSIS

Confirmation that marginal minima are found

The behavior of the minimum eigenvalue in each case is consistent with a power law in N asymptotically approaching zero. This is evidenced for a representative set of data from

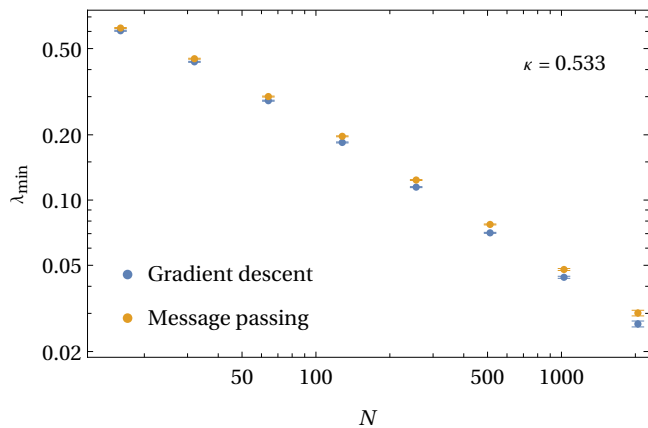


FIG. 1. Log-log plot of the minimum eigenvalue λ_{\min} as a function of N measured in our experiments for $\kappa = 0.533$.

$\kappa = 0.533$ in Fig. 1. We concluded from this data that the points found by our algorithms are indeed asymptotically marginal.

Fitting the asymptotic energy

The results in the main text are extrapolations of the raw measurements above. Since good extrapolation is a tricky problem, we share in detail our procedure for estimating the asymptotic results.

First, the mean-field analysis predicts that at $\kappa = 0$ and $\kappa = 1$, marginal minima only appear at a single energy. Therefore, both algorithms should also approach that energy. Fig. 2 shows the approach of the measured performance of both algorithms to the predicted threshold energy in these two cases, and the results are consistent with power-law approaches that are the same for the two algorithms but different at different κ . The measured exponents are $\gamma_0 = 0.624 \pm 0.004$ and $\gamma_1 = 0.718 \pm 0.007$ for $\kappa = 0$ and $\kappa = 1$, respectively.

We therefore have a reasonable expectation that the convergence of the energy of each algorithm to its asymptotic value should be well-described by a power law depending on κ . We fit to each set of data the function

$$E(N) = E_{\text{alg}} + (a_0 + a_1 N + a_2 N^2)^{-\gamma/2} \quad (4)$$

which is a truncated expansion in large N about the asymptotic value. The values of the exponent γ resulting from this fit can be found in Fig. 3, where they are also compared with the fit at $\kappa = 0$ and 1 that used knowledge of the asymptotic energy. The values of the exponent predicted by these fits is roughly consistent with their more precise value at these two points.

Table VI shows the values of the energy that were plotted in the figure in the main text, both from the mean-field prediction and from these asymptotic fits. For another perspective on the relationship between our data, fits, and the mean-field predictions, Fig. 4 shows the approach of the algorithmic performance to the mean-field threshold at an intermediate value $\kappa = 0.533$. There, neither algorithm appears to asymptotically

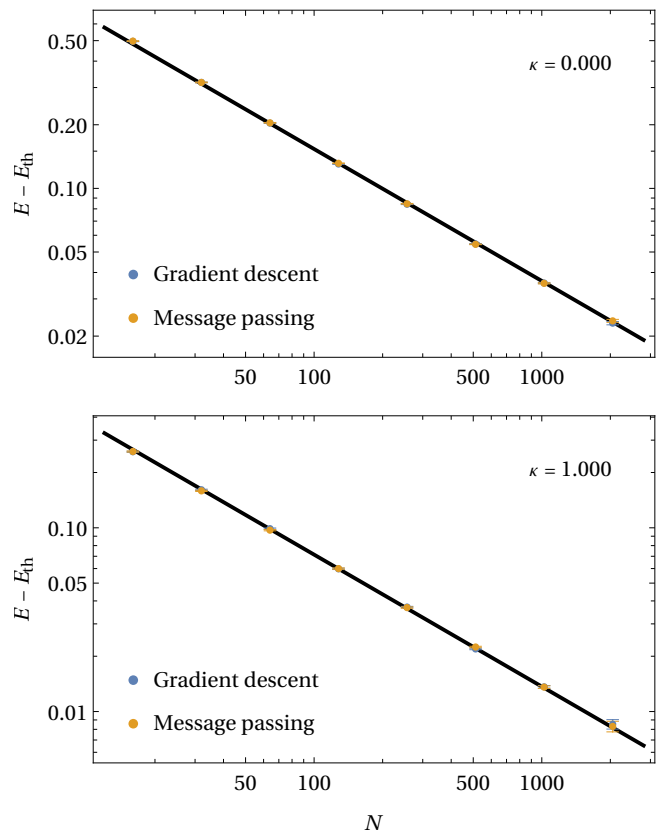


FIG. 2. The approach of algorithmic performance to the mean-field predicted threshold energy of the model for $\kappa = 0.000$ and $\kappa = 1.000$, where marginal minima are predicted to exist at only one energy. The black lines show power-law fits with exponents $\gamma_0 = 0.624 \pm 0.004$ and $\gamma_1 = 0.718 \pm 0.007$, respectively.

approach the threshold energy, instead approaching energies above and below.

-
- [1] P. Wolfe, Convergence conditions for ascent methods, *SIAM Review* **11**, 226 (1969).
 - [2] E. Subag, Following the ground states of full-RSB spherical spin glasses, *Communications on Pure and Applied Mathematics* **74**, 1021 (2020).
 - [3] J. Kent-Dobias, https://github.com/kentdobias/least_squares/releases/tag/marginal_paper.
 - [4] O. Tange, GNU parallel: The command-line power tool, ;login: The USENIX Magazine **36**, 42 (2011).

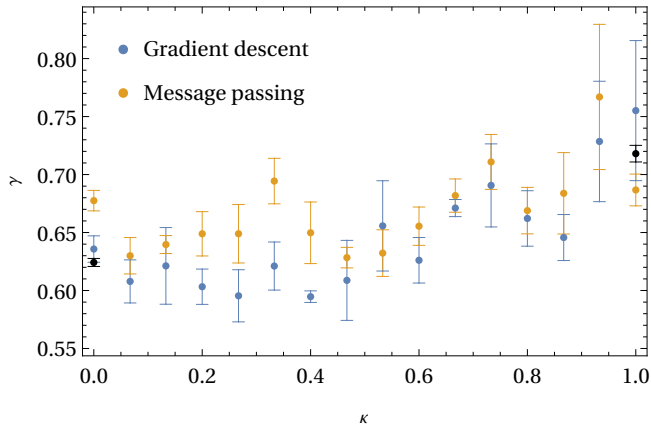


FIG. 3. The fit value of the exponent γ for the two algorithms at all values of κ . The black points for $\kappa = 0$ and 1 are the results of our fit of the exponent in Fig. 2 where the asymptotic value of the energy was an input in the fit.

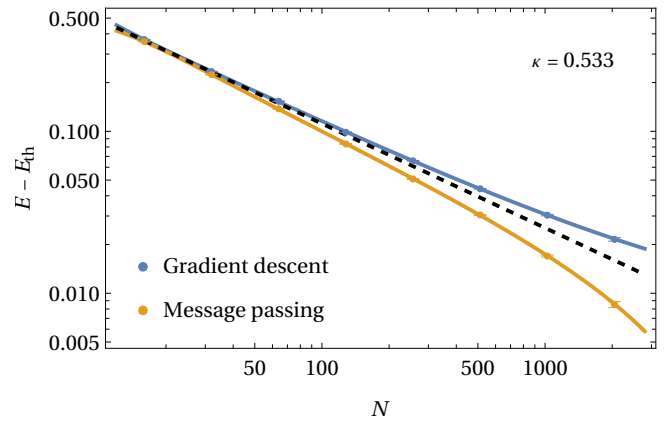


FIG. 4. The approach of algorithmic performance to the mean-field predicted threshold energy of the model for $\kappa = 0.533$. The solid lines show our fit to the data, while the dashed line shows a pure power-law whose exponent is the same as the fits.

κ	$N = 16$	$N = 32$	$N = 64$	$N = 128$	$N = 256$	$N = 512$	$N = 1024$	$N = 2048$
0.000	10000	10000	10000	10000	10000	10000	2712	296
0.067	10000	10000	10000	10000	10000	10000	1706	227
0.133	10000	10000	10000	10000	10000	10000	1799	242
0.200	10000	10000	10000	10000	10000	10000	1820	254
0.267	10000	10000	10000	10000	10000	10000	1897	262
0.333	10000	10000	10000	10000	10000	10000	1990	274
0.400	10000	10000	10000	10000	10000	10000	2026	284
0.467	10000	10000	10000	10000	10000	10000	2132	291
0.533	10000	10000	10000	10000	10000	10000	2140	266
0.600	10000	10000	10000	10000	10000	10000	2270	295
0.667	10000	10000	10000	10000	10000	10000	2390	297
0.733	10000	10000	10000	10000	10000	10000	1898	319
0.800	10000	10000	10000	10000	10000	10000	1994	365
0.867	10000	10000	10000	10000	10000	10000	2390	296
0.933	10000	10000	10000	10000	10000	10000	2669	342
1.000	10000	10000	10000	10000	10000	10000	3570	256

TABLE I. Number of independent samples in each of the measurements reported here.

κ	$N = 16$	$N = 32$	$N = 64$	$N = 128$	$N = 256$	$N = 512$	$N = 1024$	$N = 2048$
0.000	-0.90798(173)	-1.08681(119)	-1.20043(78)	-1.27367(49)	-1.31994(31)	-1.34949(19)	-1.36840(23)	-1.38103(42)
0.067	-0.89882(173)	-1.07332(120)	-1.18424(79)	-1.25510(51)	-1.29939(32)	-1.32750(19)	-1.34606(29)	-1.35870(55)
0.133	-0.89681(176)	-1.06173(120)	-1.16618(80)	-1.23453(51)	-1.27791(32)	-1.30519(20)	-1.32412(30)	-1.33497(52)
0.200	-0.88798(177)	-1.04550(122)	-1.14865(80)	-1.21303(51)	-1.25469(33)	-1.28126(21)	-1.29835(31)	-1.31045(52)
0.267	-0.87660(180)	-1.02661(121)	-1.12894(80)	-1.19104(52)	-1.23022(33)	-1.25646(21)	-1.27275(30)	-1.28363(56)
0.333	-0.86618(179)	-1.01193(123)	-1.10826(82)	-1.16761(52)	-1.20546(34)	-1.23027(21)	-1.24608(30)	-1.25565(55)
0.400	-0.85336(179)	-0.99313(122)	-1.08574(81)	-1.14308(53)	-1.17929(33)	-1.20294(22)	-1.21826(30)	-1.22829(54)
0.467	-0.83896(180)	-0.97360(124)	-1.06183(82)	-1.11717(52)	-1.15093(34)	-1.17439(21)	-1.18867(31)	-1.19803(50)
0.533	-0.82028(179)	-0.95490(121)	-1.03533(80)	-1.09002(52)	-1.12292(33)	-1.14447(21)	-1.15830(30)	-1.16714(52)
0.600	-0.80336(180)	-0.92861(122)	-1.01045(81)	-1.06132(52)	-1.09318(33)	-1.11376(21)	-1.12646(29)	-1.13555(55)
0.667	-0.78234(178)	-0.90690(122)	-0.98288(80)	-1.03123(52)	-1.06153(33)	-1.08069(21)	-1.09269(27)	-1.10042(46)
0.733	-0.76018(180)	-0.87895(120)	-0.95269(80)	-0.99954(51)	-1.02951(33)	-1.04739(21)	-1.05858(31)	-1.06641(48)
0.800	-0.73753(179)	-0.85193(122)	-0.92277(80)	-0.96739(51)	-0.99464(33)	-1.01148(21)	-1.02201(30)	-1.02932(47)
0.867	-0.71079(177)	-0.81968(120)	-0.89046(80)	-0.93342(51)	-0.95877(32)	-0.97430(20)	-0.98450(26)	-0.99067(45)
0.933	-0.68189(179)	-0.79114(121)	-0.85529(78)	-0.89637(51)	-0.92134(32)	-0.93553(20)	-0.94471(25)	-0.95055(41)
1.000	-0.65664(179)	-0.75501(121)	-0.81712(80)	-0.85626(52)	-0.87901(32)	-0.89415(21)	-0.90243(22)	-0.90752(51)

TABLE II. Measured data for the energy E_{gd} achieved by gradient descent optimization from a random initial condition on the maximum sum-of-squares problem with $f(q) = \kappa q + (1 - \kappa)q^2$ and $\alpha = \frac{1}{8}$. Each column contains the mean value of many experiments on independent disorder, while the parentheses give the standard uncertainty of the mean in the last digits.

κ	$N = 16$	$N = 32$	$N = 64$	$N = 128$	$N = 256$	$N = 512$	$N = 1024$	$N = 2048$
0.000	-0.90656(173)	-1.08690(120)	-1.19982(78)	-1.27261(49)	-1.31950(31)	-1.34970(19)	-1.36852(22)	-1.38044(39)
0.067	-0.91469(172)	-1.08552(116)	-1.19829(77)	-1.26681(48)	-1.31157(29)	-1.33963(18)	-1.35771(25)	-1.36920(42)
0.133	-0.91405(174)	-1.07836(117)	-1.18447(76)	-1.25167(46)	-1.29430(29)	-1.32138(17)	-1.33857(24)	-1.35000(41)
0.200	-0.91057(173)	-1.06693(117)	-1.16777(73)	-1.23270(46)	-1.27352(28)	-1.29962(17)	-1.31580(24)	-1.32705(38)
0.267	-0.89521(172)	-1.05252(116)	-1.14785(75)	-1.21030(46)	-1.25002(29)	-1.27478(17)	-1.29076(23)	-1.30160(36)
0.333	-0.88474(171)	-1.03517(115)	-1.12680(74)	-1.18710(46)	-1.22476(28)	-1.24881(17)	-1.26356(23)	-1.27324(38)
0.400	-0.86774(173)	-1.01317(116)	-1.10325(75)	-1.16232(46)	-1.19740(28)	-1.22014(17)	-1.23465(23)	-1.24375(36)
0.467	-0.85316(170)	-0.98973(115)	-1.07897(74)	-1.13361(47)	-1.16786(28)	-1.18933(17)	-1.20336(22)	-1.21201(36)
0.533	-0.83058(170)	-0.96488(117)	-1.05088(75)	-1.10509(46)	-1.13785(28)	-1.15823(17)	-1.17169(22)	-1.18014(36)
0.600	-0.81277(173)	-0.93960(116)	-1.02260(74)	-1.07325(46)	-1.10527(29)	-1.12487(17)	-1.13713(22)	-1.14542(36)
0.667	-0.78874(175)	-0.91342(117)	-0.99298(75)	-1.04123(47)	-1.07146(29)	-1.08986(18)	-1.10157(22)	-1.10844(35)
0.733	-0.76714(176)	-0.88650(118)	-0.96093(77)	-1.00723(47)	-1.03656(29)	-1.05406(18)	-1.06479(25)	-1.07188(35)
0.800	-0.73947(179)	-0.85407(117)	-0.92827(77)	-0.97263(48)	-0.99904(30)	-1.01608(19)	-1.02627(24)	-1.03263(35)
0.867	-0.70943(174)	-0.82420(119)	-0.89440(77)	-0.93470(48)	-0.96119(30)	-0.97666(19)	-0.98654(24)	-0.99250(39)
0.933	-0.68125(178)	-0.79198(119)	-0.85592(78)	-0.89678(50)	-0.92221(31)	-0.93639(20)	-0.94523(23)	-0.95106(37)
1.000	-0.65594(183)	-0.75720(122)	-0.81898(80)	-0.85608(51)	-0.87925(32)	-0.89360(21)	-0.90247(22)	-0.90775(55)

TABLE III. Measured data for the energy E_{mp} achieved by approximate message passing optimization from a random initial condition on the maximum sum-of-squares problem with $f(q) = \kappa q + (1 - \kappa)q^2$ and $\alpha = \frac{1}{8}$. Each column contains the mean value of many experiments on independent disorder, while the parentheses give the standard uncertainty of the mean in the last digits.

κ	$N = 16$	$N = 32$	$N = 64$	$N = 128$	$N = 256$	$N = 512$	$N = 1024$	$N = 2048$
0.000	0.71936(421)	0.51324(281)	0.33927(181)	0.21732(115)	0.13387(70)	0.08259(44)	0.05023(51)	0.03129(93)
0.067	0.70286(404)	0.50420(272)	0.33152(176)	0.21167(112)	0.13254(69)	0.08093(42)	0.04881(62)	0.02991(104)
0.133	0.69834(400)	0.49053(265)	0.32481(173)	0.20872(109)	0.13008(68)	0.07968(42)	0.04958(62)	0.03187(106)
0.200	0.68035(390)	0.48309(260)	0.31915(167)	0.20267(107)	0.12623(65)	0.07833(40)	0.04735(58)	0.02957(99)
0.267	0.66124(375)	0.46599(250)	0.31318(165)	0.19987(104)	0.12447(65)	0.07774(41)	0.04772(56)	0.02979(94)
0.333	0.65032(368)	0.45774(245)	0.30733(162)	0.19671(102)	0.12219(64)	0.07548(39)	0.04559(52)	0.02763(90)
0.400	0.63585(355)	0.45019(241)	0.30042(156)	0.19179(100)	0.12026(63)	0.07400(38)	0.04523(52)	0.02768(86)
0.467	0.62176(353)	0.44066(235)	0.29470(154)	0.18781(98)	0.11631(61)	0.07244(38)	0.04560(51)	0.02669(79)
0.533	0.60421(333)	0.43434(227)	0.28738(149)	0.18442(95)	0.11472(59)	0.07059(36)	0.04402(48)	0.02682(84)
0.600	0.59116(332)	0.42272(221)	0.28278(147)	0.18163(93)	0.11263(58)	0.07013(36)	0.04386(47)	0.02706(79)
0.667	0.57549(315)	0.41720(218)	0.27889(142)	0.17834(92)	0.11116(57)	0.06851(36)	0.04251(44)	0.02557(76)
0.733	0.56843(315)	0.40670(209)	0.27253(140)	0.17377(90)	0.10984(56)	0.06851(35)	0.04148(49)	0.02482(67)
0.800	0.56446(303)	0.40596(211)	0.26942(138)	0.17280(89)	0.11005(57)	0.06794(35)	0.04234(49)	0.02542(71)
0.867	0.56650(299)	0.40422(209)	0.26579(139)	0.17300(89)	0.10909(56)	0.06820(35)	0.04289(44)	0.02695(75)
0.933	0.57989(310)	0.40681(214)	0.26445(138)	0.17036(88)	0.10888(56)	0.06789(34)	0.04303(42)	0.02703(71)
1.000	0.62006(347)	0.40045(221)	0.25863(144)	0.16637(92)	0.10520(58)	0.06789(37)	0.04245(39)	0.02644(92)

TABLE IV. Measured data for the minimum eigenvalue $\lambda_{\text{min,gd}}$ of the Hessian matrix at the optimum found by gradient descent optimization from a random initial condition on the maximum sum-of-squares problem with $f(q) = \kappa q + (1 - \kappa)q^2$ and $\alpha = \frac{1}{8}$. Each column contains the mean value of many experiments on independent disorder, while the parentheses give the standard uncertainty of the mean in the last digits.

κ	$N = 16$	$N = 32$	$N = 64$	$N = 128$	$N = 256$	$N = 512$	$N = 1024$	$N = 2048$
0.000	0.71938(417)	0.51263(279)	0.34091(182)	0.21405(113)	0.13347(70)	0.08284(43)	0.05028(50)	0.02905(85)
0.067	0.71827(409)	0.51024(272)	0.34111(179)	0.21664(113)	0.13767(71)	0.08433(44)	0.05112(62)	0.03199(115)
0.133	0.72265(410)	0.51023(270)	0.33633(174)	0.21749(110)	0.13659(70)	0.08440(43)	0.05343(64)	0.03070(108)
0.200	0.70819(393)	0.50095(265)	0.33180(170)	0.21504(109)	0.13350(68)	0.08465(43)	0.05173(61)	0.03275(110)
0.267	0.68157(380)	0.49125(257)	0.32417(166)	0.21083(106)	0.13159(66)	0.08284(41)	0.05149(59)	0.03264(106)
0.333	0.68096(372)	0.48421(251)	0.32048(165)	0.20799(104)	0.13008(65)	0.08147(41)	0.05059(56)	0.03199(98)
0.400	0.65990(362)	0.47288(244)	0.31322(161)	0.20207(102)	0.12839(65)	0.08071(40)	0.05020(54)	0.02974(89)
0.467	0.64214(344)	0.45833(236)	0.30726(153)	0.19883(100)	0.12532(63)	0.07867(39)	0.04781(51)	0.03064(91)
0.533	0.62187(333)	0.44892(227)	0.30034(151)	0.19685(97)	0.12373(60)	0.07717(38)	0.04781(51)	0.03011(90)
0.600	0.60851(322)	0.43718(223)	0.29416(148)	0.19112(94)	0.12063(59)	0.07575(37)	0.04748(49)	0.03010(83)
0.667	0.59020(316)	0.42813(215)	0.29062(144)	0.18506(91)	0.11833(58)	0.07433(36)	0.04598(44)	0.02876(82)
0.733	0.58186(311)	0.42092(214)	0.28442(140)	0.18296(89)	0.11722(57)	0.07245(36)	0.04536(50)	0.02778(77)
0.800	0.57098(302)	0.41448(208)	0.27944(139)	0.18020(89)	0.11374(55)	0.07243(35)	0.04496(49)	0.02855(72)
0.867	0.56885(293)	0.41109(209)	0.27692(138)	0.17709(86)	0.11344(55)	0.07123(34)	0.04510(45)	0.02903(81)
0.933	0.58620(308)	0.41033(211)	0.26824(135)	0.17506(86)	0.11218(55)	0.07045(35)	0.04371(40)	0.02813(70)
1.000	0.62062(347)	0.40689(224)	0.26055(145)	0.16625(92)	0.10557(58)	0.06708(36)	0.04262(38)	0.02829(102)

TABLE V. Measured data for the minimum eigenvalue $\lambda_{\min,mp}$ of the Hessian matrix at the optimum found by approximate message passing optimization from a random initial condition on the maximum sum-of-squares problem with $f(q) = \kappa q + (1 - \kappa)q^2$ and $\alpha = \frac{1}{8}$. Each column contains the mean value of many experiments on independent disorder, while the parentheses give the standard uncertainty of the mean in the last digits.

κ	E_{\max}	E_{maj}	E_{gd}	E_{th}	E_{mp}	E_{\min}	E_{gs}
0.000	-1.4040575	-1.4040575	-1.4028(9)	-1.4040575	-1.4004(6)	-1.4040575	-1.4413071
0.067	-1.3534309	-1.3756461	-1.3812(16)	-1.3811572	-1.3905(12)	-1.3982616	-1.4140567
0.133	-1.3188326	-1.3475583	-1.3571(26)	-1.3576074	-1.3697(6)	-1.3767883	-1.3862994
0.200	-1.2868229	-1.3187015	-1.3319(13)	-1.3326088	-1.3452(12)	-1.3513189	-1.3571483
0.267	-1.2565960	-1.2895687	-1.3052(19)	-1.3064171	-1.3193(15)	-1.3234285	-1.3269697
0.333	-1.2279759	-1.2606161	-1.2751(15)	-1.2793533	-1.2881(10)	-1.2940793	-1.2961899
0.400	-1.1997200	-1.2307909	-1.2481(4)	-1.2504947	-1.2598(15)	-1.2626306	-1.2638278
0.467	-1.1719637	-1.2004436	-1.2164(24)	-1.2201357	-1.2284(5)	-1.2296515	-1.2302922
0.533	-1.1448189	-1.1700419	-1.1822(21)	-1.1886609	-1.1954(11)	-1.1957413	-1.1960622
0.600	-1.1171307	-1.1383232	-1.1506(12)	-1.1550201	-1.1588(8)	-1.1599089	-1.1600522
0.667	-1.0888977	-1.1056071	-1.1131(3)	-1.1195931	-1.1204(6)	-1.1226685	-1.1227239
0.733	-1.0600370	-1.0722906	-1.0775(14)	-1.0828870	-1.0821(8)	-1.0846003	-1.0846179
0.800	-1.0289907	-1.0367316	-1.0405(10)	-1.0437575	-1.0436(8)	-1.0445305	-1.0445345
0.867	-0.9952971	-0.9990875	-1.0018(9)	-1.0027533	-1.0026(13)	-1.0029953	-1.0029958
0.933	-0.9584445	-0.9595729	-0.9585(15)	-0.9605787	-0.9581(15)	-0.9606113	-0.9606114
1.000	-0.9160000	-0.9160000	-0.9151(15)	-0.9160000	-0.9169(4)	-0.9160000	-0.9160000

TABLE VI. Significant energy values plotted in the main text. Numbers without uncertainty are the result of a mean-field calculation and have arbitrary precision. Numbers with uncertainty are the result of an extrapolation of data to infinite N described in the text of this supplement.